ELSEVIER

Journal of Alloys and Compounds 469 (2009) 445–450

Journal of ALLOYS AND COMPOUNDS

www.elsevier.com/locate/jallcom

Effect of pre-strain on microstructure and stress corrosion cracking of over-aged 7050 aluminum alloy

D. Wang, Z.Y. Ma *

Institute of Metal Research, Chinese Academy of Sciences, 72 Wenhua Road, Shenyang 110016, China

Received 23 November 2007; received in revised form 28 January 2008; accepted 30 January 2008
Available online 12 March 2008

Abstract

The effect of pre-strain on the microstructure and stress corrosion cracking of over-aged 7050 aluminum alloy was investigated. In the over-aged 7050 alloy the η- ($MgZn_2$) phase was the main precipitates. The size of the η-phase particles within grains increased with increasing the pre-strain deformation, which resulted in the reduction in the mechanical strength of the alloy. Compared to that of the sample without pre-strain, the precipitates in the grain boundaries of pre-strained samples became smaller and tended to form relatively continuous distribution with increasing the pre-strain percents, resulting in a continuous decrease in the stress corrosion cracking (SCC) resistance.

Keywords: Aluminum; Stress corrosion cracking; Pre-strain; Grain boundaries; Microstructure

1. Introduction

7000 series aluminum alloys are widely used in aircraft structures due to the high strength and low density [1]. The high strength of the 7000 series alloys is due to the fine and uniformly distributed precipitates in the matrix which precipitate during the artificial aging. The usual precipitation sequence of the 7000 series Al alloys can be summarized as: Solid solution–GP zones–Metastable η′–Stable η ($MgZn_2$) [2–4]. In the peak aged (T6) 7000 series aluminum alloys, the η′-phase is the main precipitates. However, for the over-aging temper (T7×) the main precipitate is the η-phase [5–7].

The stress corrosion cracking (SCC) resistance is of practical importance for the industrial applications of the 7000 series aluminum alloys. Until the middle of the 1970s, the mechanism of the SCC was thought to be associated with simple anodic dissolution of the grain boundary region because the SCC is frequently intergranular for these alloys [1]. However, the subsequent investigations indicated that the hydrogen which induced hydrogen embrittlement plays an important role in this process [8,9]. Recently, it was reported that both anodic dissolution and hydrogen embrittlement operated in the SCC process [10]. Furthermore, it was suggested that the Mg segregation also plays an important role in the SCC process [11,12]. Although the SCC mechanism is not completely understood in these alloys, many efforts have been made to correlate the heat treatment and resultant microstructure with the SCC behavior of the alloys [13–15]. The major microstructural features that affect the SCC resistance are the grain boundary precipitates (GBP). The SCC resistance could be improved by increasing both size and interval of the GBP. For the over-aged 7000 series alloys, the grain boundaries are characterized by large and discontinuous precipitates. Therefore the SCC susceptibility of the 7000 series alloys could be significantly improved under over-aged condition.

A pre-strain is usually applied to the 7000 series alloys in the as-quenched state to relieve quench-induced internal stress [16]. It is widely recognized that the presence of dislocations which are generated in the pre-strain process greatly influences the subsequent precipitation process, thereby affecting the mechanical properties of age-hardened aluminum alloys. For the 7000 series alloys, the pre-strain usually results in the generation of equilibrium phase η ($MgZn_2$) on the dislocation network and therefore reduces the amount of the solutes for the formation of main hardening phase η′ in the T6 temper, which decreases the mechanical strength of the alloys [17,18].

Although the effect of the pre-strain on the strength of the 7000 series alloys is well documented [17,18], there is no report so far about the influence of the pre-strain on the grain boundary

* Corresponding author. Tel.: +86 24 83978908; fax: +86 24 83978908.
E-mail address: zyma@imr.ac.cn (Z.Y. Ma).

0925-8388/$ – see front matter © 2008 Elsevier B.V. All rights reserved.
doi:10.1016/j.jallcom.2008.01.137

Table 1
Chemical compositions of 7050 Al alloy (wt.%)

Zn	6.18
Mg	2.20
Cu	2.21
Zr	0.13
Si	0.11
Fe	0.10
Al	Balance

precipitates and the SCC resistance of the 7000 series alloys. In this paper, we studied the microstructure and the SCC behavior of over-aged 7050 aluminum alloy with various pre-strain percents. The aims are (a) to examine the effect of the pre-strain percents on the microstructural evolution of high strength 7050 aluminum alloy, in particular the grain boundary precipitates and (b) to evaluate the effect of the change in the grain boundary precipitates on the SCC resistance.

2. Experimental

7050 aluminum casting was used as the raw material and the chemical composition of the alloy is shown in Table 1. 20-mm thick plates were cut from the casting and were homogenized at 470 °C for 48 h, and then quenched. The homogenized plates were hot-rolled to 6 mm at 430 °C. The rolled samples were solution treated at 470 °C for 1 h in a salt bath furnace followed by quenching in water at room temperature. Pre-straining was performed within 1 h after quenching along the rolling direction under the permanent elongation of 0%, 1%, 2% and 5%, respectively. Then all the samples were aged at 120 °C for 6 h followed by 165 °C for 16 h.

SCC resistance was evaluated using the slow strain rate test (SSRT) in the air and in an aqueous 3.5% NaCl solution with the gauge length of the specimens being completely immersed during the test. Dog-bone shaped specimens with a gauge length of 10 mm, a width of 3 mm and a thickness of 1 mm were machined from heat-treated plates with the tensile axis perpendicular to the rolling direction. Tensile tests were conducted at room temperature and a strain rate of $1 \times 10^{-6}\ s^{-1}$ by using an Instron 5848 testing machine.

The SCC susceptibility was evaluated by a ratio r_{tf}, which is calculated by [14]:

$$r_{tf} = \frac{t_{fe}}{t_{fc}} \quad (1)$$

where t_{fe} was the measurement of time-to-failure determined in the 3.5% NaCl aqueous solution and t_{fc} was the corresponding value determined in the air.

The fracture surfaces of the specimens were observed by the scanning electron microscopy (SEM). The precipitates in the over-aged samples was analyzed using the X-ray diffraction (XRD) and transmission electron microscopy (TEM). Thin foils for TEM were prepared by twin jet-polishing in 30% HNO_3, 70% ethanol solution cooled to −35 °C with liquid nitrogen at 19 V. Differential scanning calorimetry (DSC) experiments were performed on TAQ 1000. The heating rate was 10 K min^{-1}.

3. Results and discussion

Table 2 shows the tensile results of the over-aged 7050 samples with different pre-strain percents in the air and 3.5% NaCl solution at a strain rate of $1 \times 10^{-6}\ s^{-1}$. The ultimate tensile strength (UTS) of the samples tended to decrease as the pre-strain percents increased. The UTS of the sample with a pre-strain of 5% (here after referred to as 5% pre-strain sample) decreased by 32 MPa compared to that of the sample without the pre-strain (hereafter referred to as 0% pre-strain sample).

Table 2
Transverse mechanical properties of over-aged 7050 Al plate at a strain rate of $1 \times 10^{-6}\ s^{-1}$

Pre-strain (%)	UTS (MPa)		Elongation (%)	
	In air	In 3.5% NaCl	In air	In 3.5% NaCl
0	512	507	6.6	6.2
1	507	499	7.1	6.5
2	507	507	8.3	6.5
5	480	480	7.5	6

The UTS of the samples tested in the 3.5% NaCl solution were similar to that tested in air. On the other hand, the elongation-to-failure of the samples with pre-strain treatment tested in the air increased slightly compared to that of 0% pre-strain sample, which were higher than those in the 3.5% NaCl solution. Similar results were also reported in other 7000 aluminum alloys [11,17].

Fig. 1 illustrates the variation of the r_{tf} with the pre-strain percents for the over-aged 7050 samples. The r_{tf} is an index for evaluating the SCC resistance of a material. The greater the r_{tf} value, the better the SCC resistance is [14]. A r_{tf} value of 1 implies that the material exhibits no SCC susceptibility. Fig. 1 reveals that the r_{tf} value of the 0% pre-strain sample is 0.97. This means the SCC hardly occurs in this sample. Similar result was previously reported in over-aged 7050 aluminum alloys [6,14]. Furthermore, Fig. 1 shows that the r_{tf} decreases as the pre-strain percents increases, indicating that the pre-strain tended to reduce the SCC resistance of the 7050 aluminum alloy.

Fig. 2(a) presents a typical tensile fracture surface of the 0% pre-strain sample tested in the air. The fracture surface was characterized by large dimples, showing the characteristic of ductile fracture. The fracture surfaces of the samples with various pre-strain percents tested in the air were similar to that of the 0% pre-strain sample. In contrast, intergranular microvoid coalescences were found in the 0% pre-strain sample tested in the saline solution (Fig. 2(b)). This is attributed to the preferential deformation of the precipitate free zone around the grain boundary area [19]. Furthermore, some large dimples and cleav-

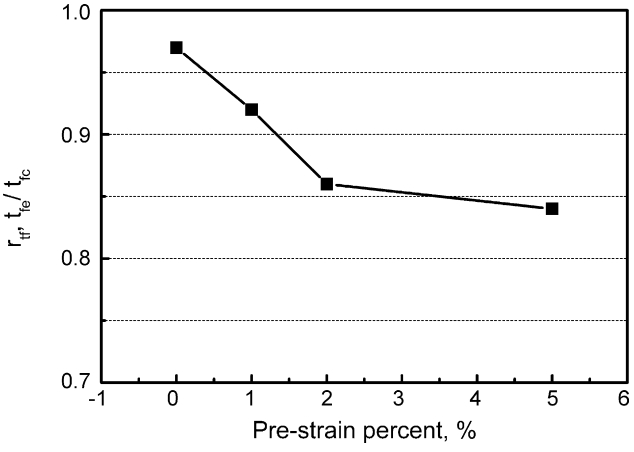

Fig. 1. Variation of r_{tf} with pre-strain percents for over-aged 7050 aluminum alloy.

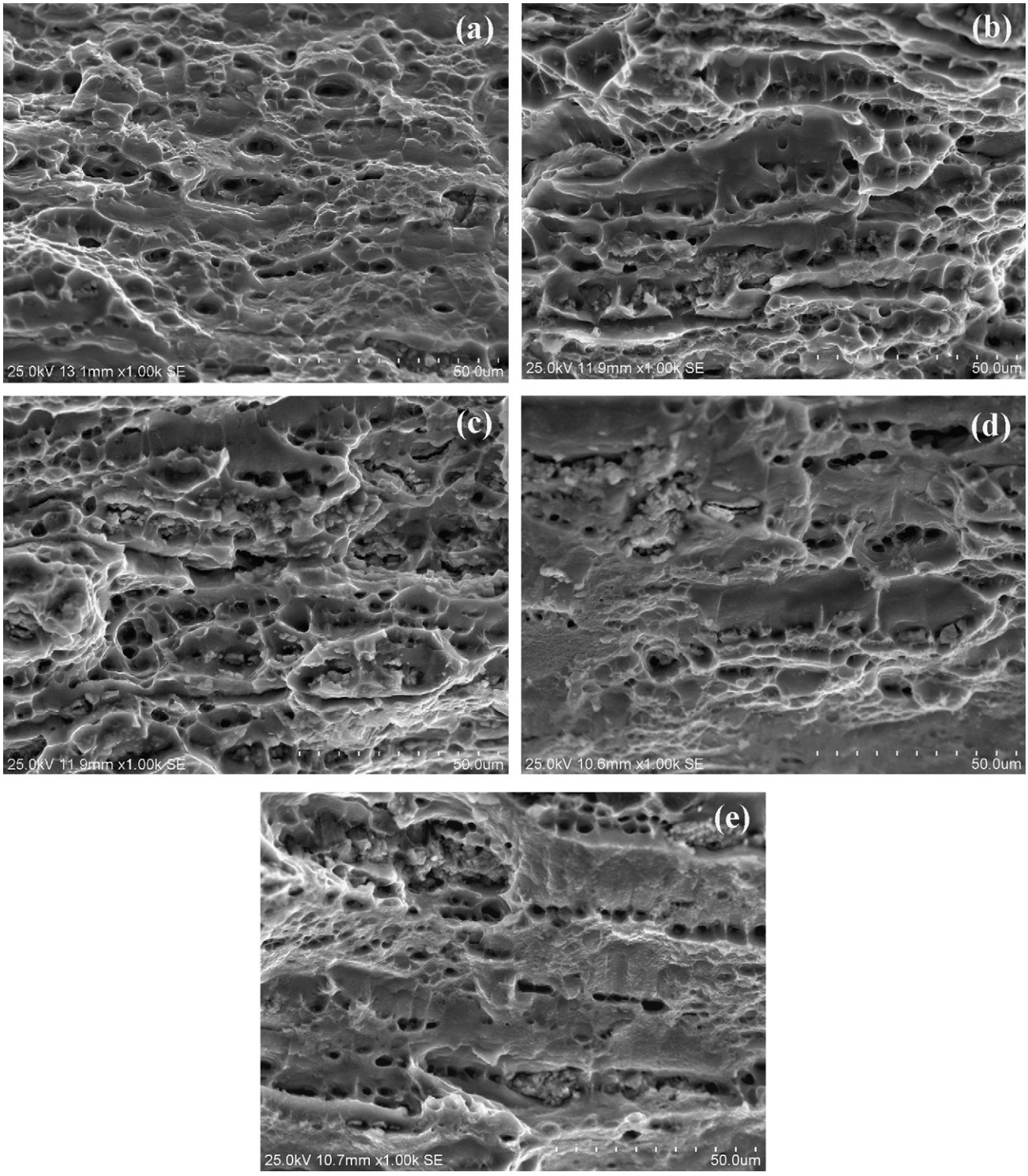

Fig. 2. SEM micrographs showing SSRT fracture surfaces of 7050 samples with (a and b) a pre-strain of 0% and (c–e) a pre-strain of 1, 2 and 5%, respectively; (a) in air and (b–e) in 3.5% NaCl solution.

age facets were also observed on the fracture surface of this sample. Fig. 2(c)–(e) shows the tensile fracture surfaces of the samples with a pre-strain of 1, 2 and 5%, respectively, tested in the saline solution. The large dimples on the fracture surface became less as the pre-strain percent increased, whereas the intergranular microvoid coalescences became more. For the 5% pre-strain sample, the dimples disappeared nearly and the fracture surface was characterized by the intergranular microvoid coalescences and cleavage facets (Fig. 2(e)). The predominance of the intergranular microvoid coalescences suggested that the grain boundaries were the preferential paths for the SCC.

It is well documented that the strength and the SCC resistance of the 7050 aluminum alloy are significantly dependent on the microstructure. In the over-aged 7050 alloy the main precipitates

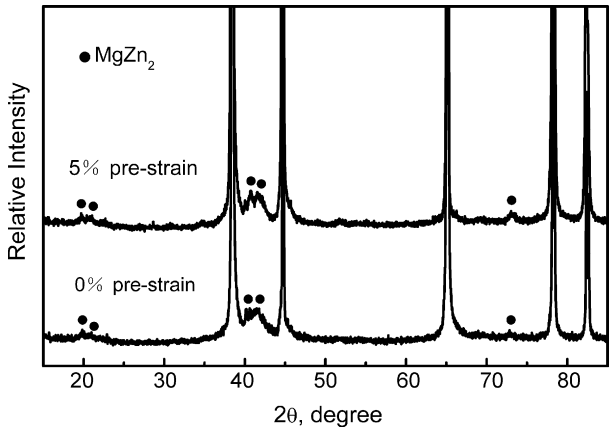

Fig. 3. X-ray diffraction patterns of 7050 samples with a pre-strain of 0 and 5%, respectively.

are the η-phase [20]. Fig. 3 shows the X-ray diffraction patterns of the samples with a pre-strain of 0 and 5%, respectively. The diffraction peaks of the η- ($MgZn_2$) phase were observed in both samples, suggesting that the η-phase was the main precipitate

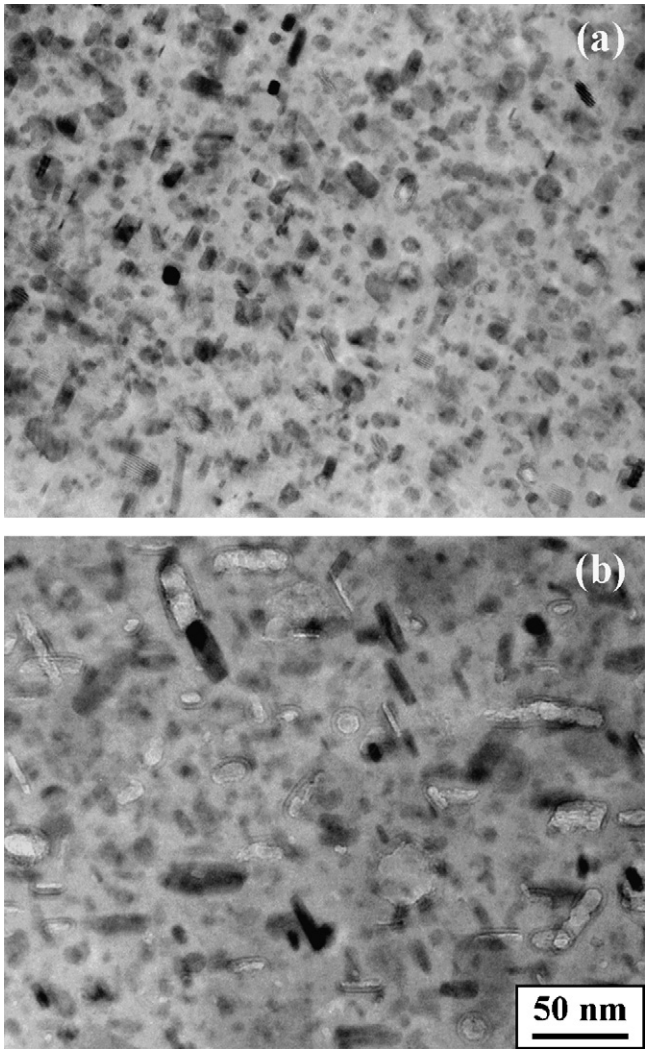

Fig. 4. TEM micrographs showing precipitates within grains of 7050 samples with a pre-strain of (a) 0% and (b) 5%.

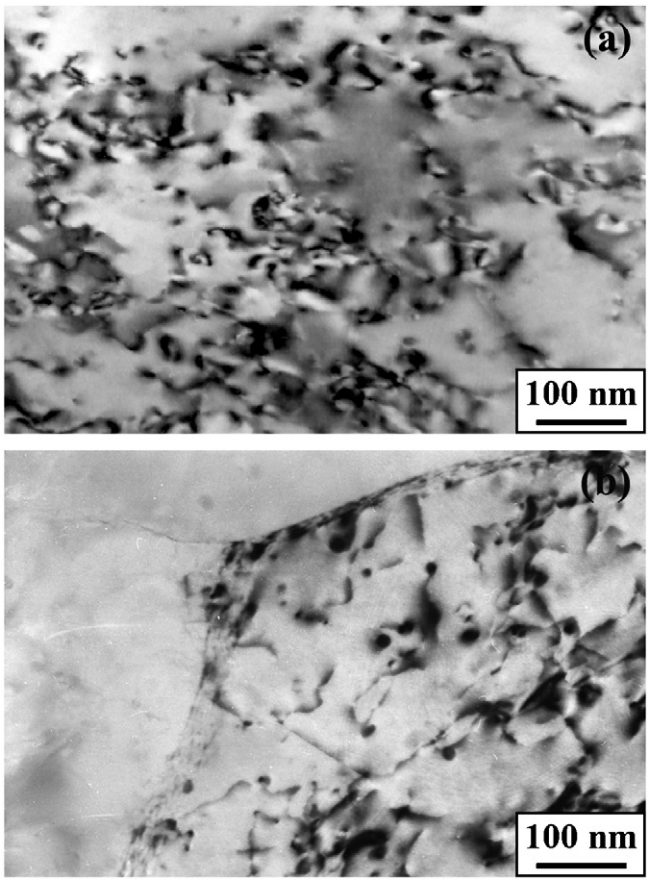

Fig. 5. TEM micrographs showing dislocations of 5% pre-strain 7050 sample prior to aging: (a) within grains and (b) around grain boundaries.

in both samples. This is consistent with the previous studies [20].

Fig. 4 shows the TEM images of the samples with a pre-strain percents of 0 and 5%, respectively. The main precipitates within the grains were the η-phase in both samples. In the 0% pre-strain sample the precipitates were homogeneously distributed. However, in the 5% pre-strain sample some coarse precipitates appeared within the grains and there were no other precipitates around these coarse precipitates. It is well known that dislo-

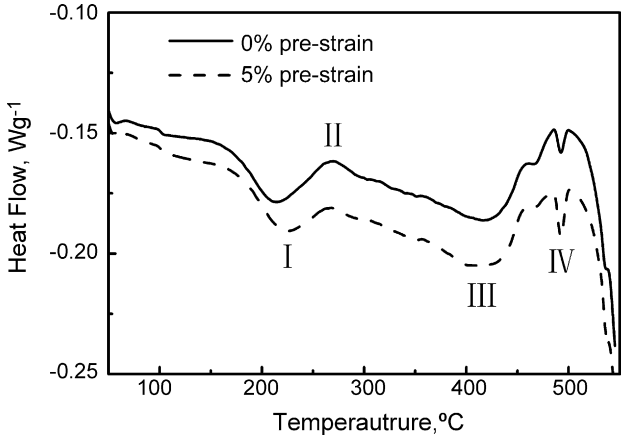

Fig. 6. DSC curves of 0 and 5% pre-strain samples.

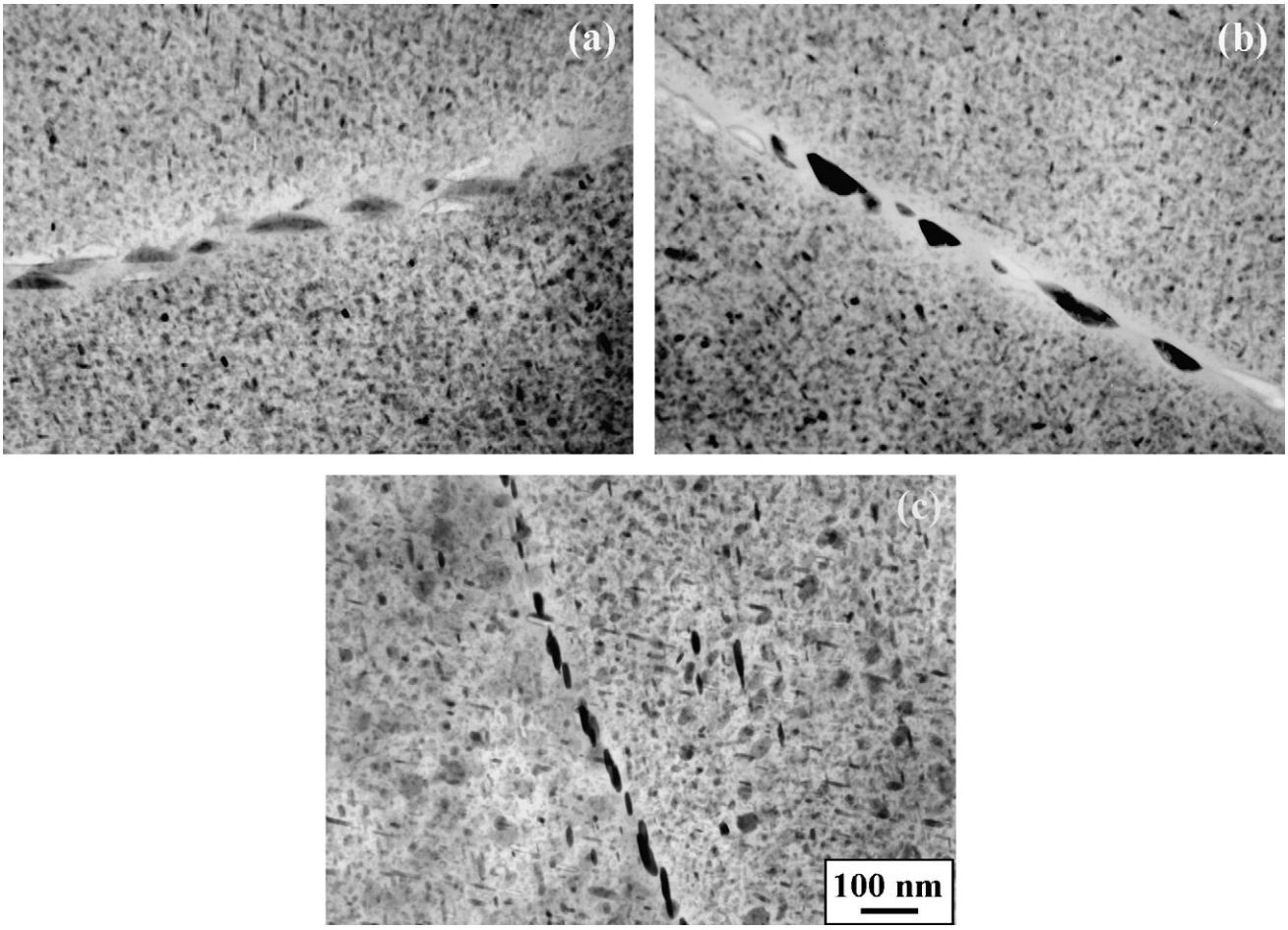

Fig. 7. TEM micrographs showing grain boundary precipitates in 7050 samples with a pre-strain of (a) 0%, (b) 1%, and (c) 5%.

cations can be generated in a metallic material during cold deformation. Fig. 5(a) shows the TEM image of the 5% pre-strain sample prior to the aging. High density of dislocations was clearly visible within the grains, without the precipitates on the dislocations. The dislocations could provide efficient sites for heterogeneous nucleation of the precipitates and they were also fast diffusion paths for the precipitation elements in the aging process [18,21].

Fig. 6 illustrates the DSC curves for the 0 and 5% pre-strain samples. Since the samples were under the over-aged condition, the formation and dissolution of GP zones were not observed in these curves. Recent studies [22,23] indicated that peak I was caused by the dissolution of the small η-phase, peak II corresponded to the coarsening of the η-phase, and peak III was due to the dissolution of the η-phase. And peak IV was associated with the dissolution of S-phase (Al_2CuMg). The DSC curves of the 0 and 5% pre-strain samples were all but same. However, it is noted that the incipient temperature of peak I in the 0% pre-strain sample was 172 °C, but that in the 5% pre-strain sample was 180 °C. This means that the average size of the fine η-phase in the 5% pre-strain sample was larger than that in the 0% pre-strain sample.

In the pre-strain samples, the dislocations provided efficient sites for heterogeneous nucleation of the η′-phase at 120 °C and accelerated the elements diffusion in the early aging process and made the η′-phase coarsen in this process. When the samples were aged at 165 °C, the η′-phase transformed to the η-phase. While some η′-phase precipitated in the dislocations network grew up and formed the coarse precipitates in the matrix, part of η′-phase transformed to η-phase directly, which increased the average size of the small η-phase. Therefore, the coarsening of η phases in the pre-strained samples reduced the density of the precipitates within the grains, leading to a reduction of the strength (Table 2).

In the over-aged 7050 alloy, the grain boundaries were characterized by the coarse and discontinuously distributed η-phase particles that exert an important effect on the SCC susceptibility of the alloy. Fig. 7 shows the TEM images of the samples with various pre-strain percents. In these samples, all the grain boundaries were decorated with the coarse and discontinuously distributed η-phase particles. The 0% pre-strain sample had the largest grain boundary precipitates. With increasing the pre-strain percents, the η-phase particles at the grain boundaries became smaller and tended to form relatively continuous distribution. The small grain boundaries particles were of benefit to the toughness of the samples [24] which resulted in that the elongation increased slightly as the pre-strain percents increased.

Fig. 5(b) shows the dislocations distributed around the grain boundaries in the 5% pre-strain sample prior to the aging. Clearly, the dislocations were also aggregated around the grain

boundaries. Similar to the situation in the grains, the dislocations in the grain boundaries also provided heterogeneous nucleation sites for the η-phase particles. Consequently, the precipitates in the grain boundaries became smaller and tended to form relatively continuous distribution (Fig. 7).

Recently, the mechanism of the SCC in the Al–Zn–Mg–Cu alloys was thought to be both anodic dissolution and hydrogen embrittlement [10]. The precipitates in the grain boundaries were Mg-rich phases in these alloys, which had the electrode potential different from the Al matrix. That would result in the anodic dissolution in the aqueous chloride solutions. Furthermore, the hydrogen in the crack tip also led to the hydrogen embrittlement in the grain boundaries. In the over-aged 7050 aluminum alloy, it is impossible to wipe off the Mg-containing η-phase particles in the grain boundaries. The large size and interparticle spacing of the grain boundary particles, as shown in Fig. 7a, decreased the anodic dissolution speed. Song et al. [11,12] reported that the element Mg in the grain boundaries had the electronegativity difference between Mg and H atom larger than that between Al and H atom. Therefore, Mg in the grain boundaries could increase the amount of hydrogen absorbed and consequently accelerate its diffusion and enhance the solution degree of hydrogen in the grain boundaries. This may result in the embrittlement of the grain boundaries and accelerate the growth of the stress corrosion cracks. The large η-phase particles in the grain boundaries in the 0% pre-strain sample could also act as the trapping sites for atomic hydrogen and created molecular hydrogen bubbles to reduce the concentration of the atomic hydrogen in the grain boundaries, therefore, the SCC occurred hardly in this sample. However, in the pre-strain samples the precipitates in the grain boundaries were smaller than those in the 0% pre-strain samples. That would increase the anodic dissolution speed, reduce the number of trapped hydrogen atoms, and increase the hydrogen atom diffusion on the grain boundaries. Therefore, the stress corrosion cracking would be easier to expand in these samples. In this case, the SCC resistance of the pre-strain samples would be significantly decreased, compared to the 0% pre-strain sample.

4. Conclusions

(1) The main precipitate in the over-aged 7050 aluminum alloy was the η- ($MgZn_2$) phase. Pre-strain caused the coarsening of the precipitates within the grains and reduced the size of the precipitates on the grain boundaries.
(2) The strength of the over-aged 7050 aluminum alloy decreased with increasing the pre-strain percents because of the precipitate coarsening within the grains.
(3) The SCC resistance of the over-aged 7050 aluminum alloy decreased with increasing the pre-strain percents because the precipitates in the grain boundaries became small and tended to form relatively continuous distribution.

Acknowledgment

The authors gratefully acknowledge the support of National Basic Research Program of China under grant no. 2005CB623708.

References

[1] J.E. Hatch (Ed.), Aluminum Properties and Physical Metallurgy, American Society for Metals, OH, 1984.
[2] G. Sha, A. Cerezo, Acta Mater. 52 (2004) 4503.
[3] N.Q. Chinh, J. Lendvai, D.H. Ping, K. Hono, J. Alloys Compd. 378 (2004) 52.
[4] M.M. Sharma, M.F. Amateau, T.J. Eden, J. Alloys Compd. 416 (2006) 135.
[5] A.F. Oliveira, M.C. de Barros, K.R. Cardoso, D.N. Travessa, Mater. Sci. Eng. A 379 (2004) 321.
[6] B.L. Ou, J.G. Yang, M.Y. Wei, Metall. Trans. 38A (2007) 1760.
[7] J. Grobner, L.L. Rokhlin, T.V. Dobatkina, R. Schmid-Fetzer, J. Alloys Compd. 443 (2007) 108.
[8] G.H. Koch, Corrosion 35 (1979) 73.
[9] G.M. Scamans, Metall. Trans. 11A (1980) 846.
[10] D. Najjar, T. Magnin, T.J. Warner, Mater. Sci. Eng. A 238 (1997) 293.
[11] R.G. Song, W. Dietzel, B.J. Zhang, W.J. Liu, M.K. Tseng, A. Atrens, Acta Mater. 52 (2004) 4727.
[12] R.G. Song, M.K. Tseng, B.J. Zhang, J. Liu, Z.H. Jin, K.S. Shin, Acta Mater. 44 (1996) 3241.
[13] M. Puiggali, A. Zielinski, J.M. Olive, E. Renauld, D. Desjardins, M. Cid, Corros. Sci. 40 (1998) 805.
[14] J.C. Lin, H.L. Liao, W.D. Jehng, C.H. Chang, S.L. Lee, Corros. Sci. 48 (2006) 3139.
[15] K. Rajan, W. Wallace, J.C. Beddoes, J. Mater. Sci. 17 (1982) 2817.
[16] A. Deschamps, Y. Brechet, P. Guyot, F. Livet, Z. Metallkd. 88 (1997) 601.
[17] G. Waterloo, V. Hansen, J. Gjonnes, S.R. Skjervold, Mater. Sci. Eng. A303 (2001) 226.
[18] A. Deschamps, F. Livet, Y. Brechet, Acta Mater. 47 (1999) 281.
[19] M. Bobby Kannan, V.S. Raja, J. Mater. Sci. 41 (2006) 5495.
[20] G. Sha, A. Cerezo, Surf. Interf. Anal. 36 (2004) 564.
[21] M. Talianker, B. Cina, Metall. Trans. 20A (1989) 2087.
[22] M.J. Starink, Int. Mater. Rev. 49 (2004) 191.
[23] M.J. Starink, S.C. Wang, Metall. Acta Mater. 51 (2003) 5131.
[24] D. Dumont, A. Deschamps, Y. Brechet, Mater. Sci. Eng. A356 (2003) 326.